JOC*Article*

A Theoretical Investigation of the $Co(CO)_4^-$-Catalyzed Carbonylative Ring Expansion of *N*-Benzoyl-2-methylaziridine to *β*-Lactams: Reaction Mechanism and Effect of Substituent at the Aziridine C_α Atom

Diego Ardura and Ramón López*

Departamento de Química Física y Analítica, Universidad de Oviedo, Julián Clavería, 8; E-33006 Oviedo, Spain

rlopez@uniovi.es

Received December 9, 2006

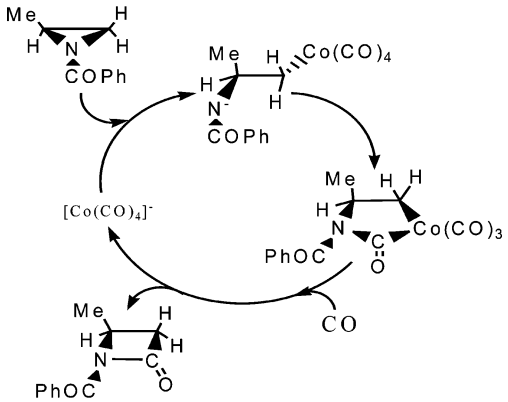

The reaction mechanism of the $Co(CO)_4^-$-catalyzed carbonylative ring expansion of *N*-benzoyl-2-methylaziridine to afford *N*-benzoyl-4-methyl-2-azetidinone and *N*-benzoyl-3-methyl-2-azetidinone was investigated by using the B3LYP density functional theory methodology in conjunction with the conductor polarizable continuum model/united atom Kohm−Sham method to take into account solvent effects. Computations predict that the most favorable reaction mechanism differs from the experimental proposals except for the nucleophilic ring-opening step, which is the rate-determining one. The regioselectivity and stereospecificity experimentally observed is explained in terms of the located reaction mechanism. The substitution of the methyl group at the carbon α of aziridine by the phenyl one gives rise to the obtaining of an only product that corresponds to the CO insertion into the C(substituted)−N bond in accordance with experimental findings. When the ethyl group replaces the methyl one the CO insertion occurs into the two C−N bonds, but the regioselectivity of the process is higher than that of the methyl substituent.

Introduction

Since the elucidation of the structure of penicillin by Crowfoot-Hodgkin et al. in 1945,[1] *β*-lactams have become the center of attention for many synthetic, medicinal, and theoretical chemists and biologists due to their utility as synthetic intermediates and to their biological activity.[2−11] As a consequence, many chemical methods for the production of *β*-lactams have been proposed.[8,9] One of these synthetic strategies is the

* Corresponding author. Phone: +34 98 5 102 967. Fax: +34 98 5 103 1255.

(1) Crowfoot, D.; Bunn, C. W.; Rogers-Low, B. W.; Turner-Jones, A. In *The Chemistry of Penicillin*; Clarke, H. T., Johnson, J. R., Robinson, R., Eds.; Princenton University Press: Princenton, New Jersey, 1949; Chapter 11, p 310.

(2) *Chemistry and Biology of β-Lactam Antibiotics*; Morin, R. B., Gorman, M., Eds.; Academic Press: New York, 1982; Vols. 1−3.

(3) Dürkheimer, W.; Blumbach, J.; Lattrell, R.; Scheunemann, K. H. *Ang. Chem., Int. Ed. Engl.* **1985**, *24*, 180.

(4) *The Chemistry of β-Lactams*, Page, M. I., Ed.; Blackie Academic & Professional: London, 1992.

(5) *The Organic Chemistry of β-Lactams*, Georg, G. I., Ed.; VCH: Weinheim, 1992.

(6) Southgate, R. *Contemp. Org. Synth.* **1994**, *1*, 417.

10.1021/jo0625249 CCC: $37.00
Published on Web 03/24/2007

SCHEME 1. Experimental Mechanistic Proposals for Aziridine Carbonylation Catalyzed by $Co(CO)_4^-$

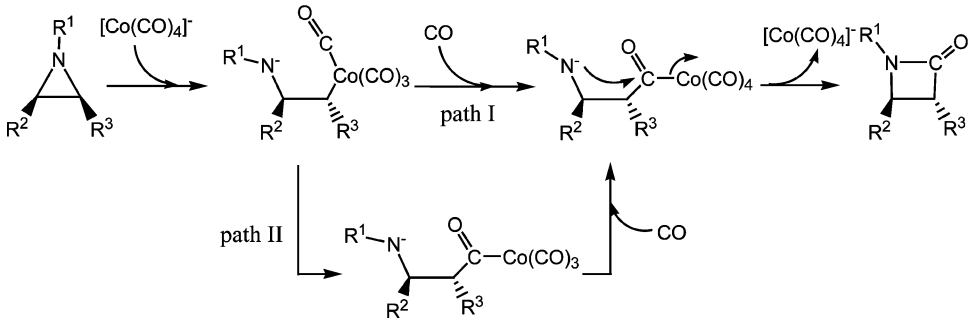

carbonylative ring expansion of aziridines catalyzed by organometallic complexes,[12−28] which presents an interesting regio-, stereo-, and enantioselectivity depending on the nature of the metal catalyst and the substituents on the ring atoms.

The first experimental studies on this kind of processes have reported that the carbonyl insertion into aziridines to afford β-lactams catalyzed by nickel,[14,16] rhodium,[15] or palladium[18] complexes proceeds with retention of configuration at the carbon atoms of the aziridine ring, i.e., *cis*-aziridines give *cis*-β-lactams, whereas *trans*-β-lactams are obtained from *trans*-aziridines. Posterior experimental works have shown that different cobalt complexes also carbonylate aziridines to generate β-lactams, but all of these processes take place with inversion of configuration at the site of attack.[20,22−26] When the $Co_2(CO)_8$ or $NaCo(CO)_4$ complexes were used as catalysts, it has been suggested[20] that the reaction would proceed via an S_N2-like mechanism (path I in Scheme 1) in which the putative active species, the $[Co(CO)_4]^-$ ion, would open the aziridine ring by attacking the least substituted carbon atom, with inversion of its configuration, to give an intermediate. Then, an external CO would insert into the C(attacked)−Co bond of this intermediate with retention of configuration to afford another open intermediate, which in turn would finally undergo a ring closure to render the β-lactam after regeneration the catalyst. When the cationic counterpart of the $[Co(CO)_4]^-$ anion is a Lewis acid, it has also been proposed another mechanistic route that differs from the above-mentioned one in the second step, the CO insertion (see path II in Scheme 1).[26] According to this suggestion, this step would take place in a two-step fashion. First, one of the carbonyl ligands of $Co(CO)_4^-$ would insert into the C(attacked)−Co bond and second, an extramolecular CO would add to the cobalt atom to regenerate the catalyst. This proposal was investigated in a mechanistic study of a related reaction by density functional theory (DFT) calculations, β-lactone formation from ethylene oxide, and CO catalyzed by the $BF_3[Co(CO)_4]$ complex.[29]

SCHEME 2. SET Mechanism Proposed for Aziridine Carbonylation Catalyzed by $Co(CO)_4^-$

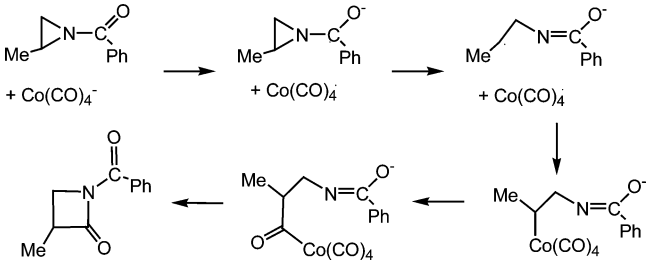

The nature of substituents on the carbon atoms of the aziridine ring determines the regioselectivity of the CO-catalyzed carbonylation reaction.[19,20,24,26] For example, for aziridines containing an alkyl substituent the insertion of CO occurs at the least hindered C−N bond,[20,26] but when a phenyl substituent is also present or replaces the alkyl one, the carbonylation of the C−N bond bearing the phenyl group takes place.[20,24] In accordance with previous experimental suggestions,[15,19,20] a recent theoretical study of the rhodium(I)-catalyzed carbonylative ring expansion of *N-tert*-butyl-2-phenylaziridine has shown that the phenyl group through its hyperconjugation interaction with the substituted C−N bond facilitates the insertion of the metal atom into this bond and subsequently that of CO.[30] Although most of these reactions lead to an only product, it is interesting to note that some carbonylative ring expansions of aziridines afford two regioisomers.[20,24,26] The first example of these is the formation of *N*-benzoyl-4-methyl-2-azetidinone and *N*-benzoyl-3-methyl-2-azetidinone from *N*-benzoyl-2-methylaziridine catalyzed by $Co_2(CO)_8$ in 1,2-dimethoxiethane (DME) at 100 °C and ∼33 atm of CO. Experimentalists have explained the obtaining of *N*-benzoyl-4-methyl-2-azetidinone through the reaction mechanism type I in Scheme 1, while a radical mechanism has been

(7) Nicolau, K. C.; Sorensen, E. J. *Classics in Total Synthesis*; VCH: Weinheim, 1996.
(8) López, R.; del Río, E.; Díaz, N.; Suárez, D.; Menéndez, M. I.; Sordo, T. L. *Recent Res. Devel. Physical Chem.* **1998**, *2*, 245.
(9) Palomo, C.; Aizpurua, J. M.; Ganboa, I.; Oiarbide, M. *Eur. J. Org. Chem.* 1999, 3223.
(10) López, R.; Menéndez, M. I.; Díaz, N.; Suárez, D.; Campomanes, P.; Sordo, T. L. *Recent Res. Devel. Physical Chem.* **2000**, *4*, 157.
(11) López, R.; Menéndez, M. I.; Díaz, N.; Suárez, D.; Campomanes, P.; Ardura, D.; Sordo, T. L. *Curr. Org. Chem.* **2006**, *10*, 805.
(12) Alper, H.; Urso, F.; Smith, D. J. H. *J. Am. Chem. Soc.* **1983**, *105*, 6737.
(13) Alper, H.; Hamel, H. *Tetrahedron Lett.* 1987, 3237.
(14) Chamchaang, W.; Pinhas, A. R. *J. Chem. Soc. Chem. Commun.* 1988, 710.
(15) Calet, S.; Urso, F.; Alper, H. *J. Am. Chem. Soc.* **1989**, *111*, 931.
(16) Chamchaang, W.; Pinhas, A. R. *J. Org. Chem.* **1990**, *55*, 2943.
(17) Spears, G. W.; Nakanishi, K.; Ohfune, Y. *Synlett* 1991, 91.
(18) Tanner, D.; Somfai, P. *Bioorg. Med. Chem. Lett.* **1993**, *3*, 2415.
(19) Khumtaveeporn, K.; Alper, H. *Acc. Chem. Res.* **1995**, *28*, 414.
(20) Piotti, M. E.; Alper, H. *J. Am. Chem. Soc.* **1996**, *118*, 111.
(21) Ley, S. V.; Middleton, B. *Chem. Commun.* 1998, 1995.
(22) Davoli, P.; Moretti, I.; Prati, F.; Alper, H. *J. Org. Chem.* **1999**, *64*, 518.
(23) Davoli, P.; Prati, F. *Heterocycles* **2000**, *53*, 2379.
(24) Davoli, P.; Forni, A.; Moretti, I.; Prati, F.; Torre, G. *Tetrahedron* **2001**, *57*, 1801.
(25) Lee, J. T.; Thomas, P. J.; Alper, H. *J. Org. Chem.* **2001**, *66*, 5424.
(26) Mahadevan, V.; Getzler, Y. D. Y. L.; Coates, G. W. *Angew. Chem., Int. Ed.* **2002**, *41*, 2781.
(27) Lu, S. M.; Alper, H. *J. Org. Chem.* **2004**, *69*, 3558.
(28) Davoli, P.; Spaggiari, A.; Ciamaroni, E.; Forni, A.; Torre, G.; Prati, F. *Heterocycles* **2004**, *63*, 2495.
(29) Molnar, F.; Luinstra, G.; Allmendinger, M.; Rieger, B. *Chem.−Eur. J.* **2003**, *9*, 1273.
(30) Ardura, D.; López, R.; Sordo, T. L. *J. Org. Chem.* **2006**, *71*, 7315.

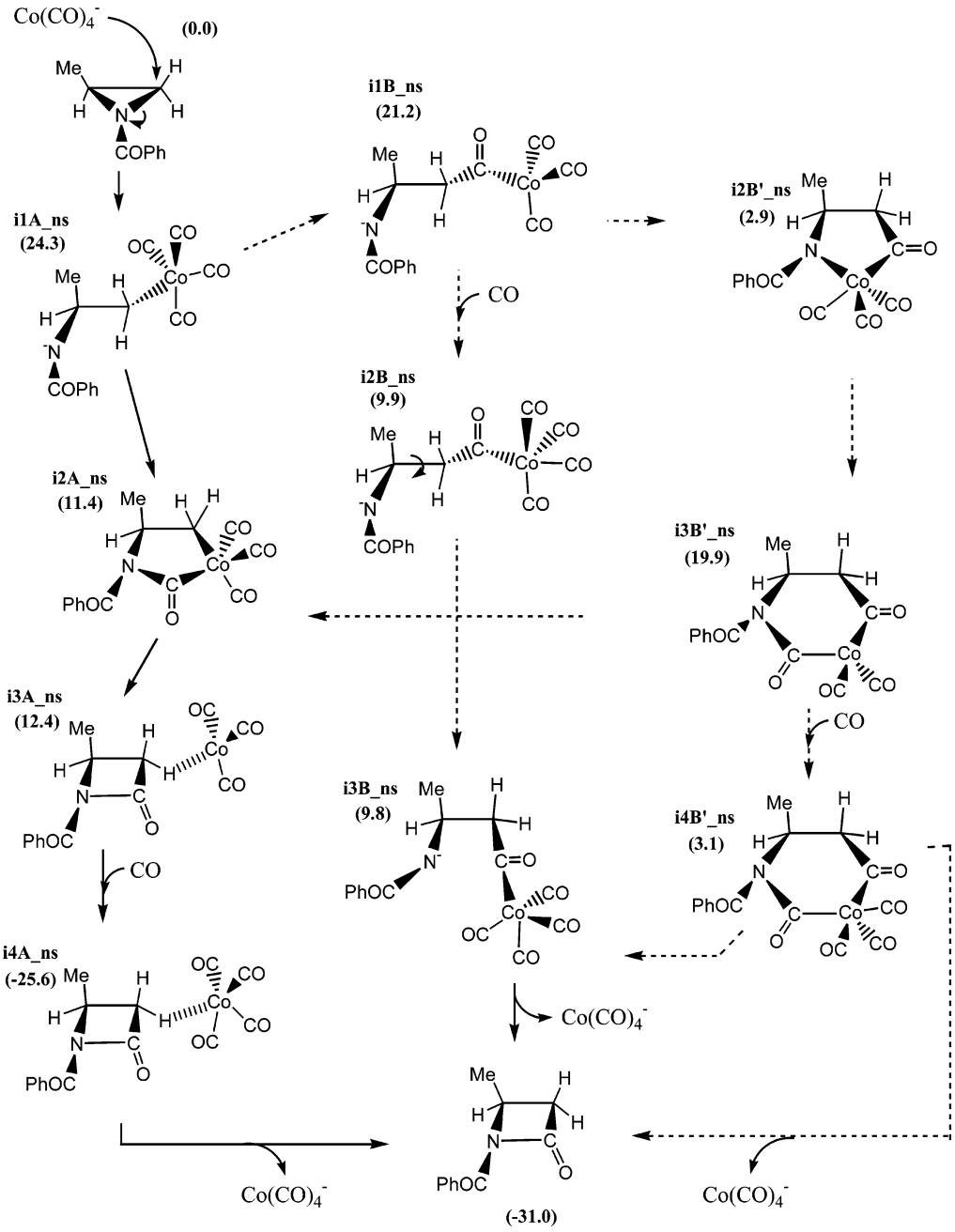

FIGURE 1. Schematic view of the different reaction mechanisms located for the carbonyl insertion into the least substituted C−N bond of (*S*)-*N*-benzoyl-2-methylaziridine catalyzed by $Co(CO)_4^-$. Only reactants, products, and intermediates are shown.

invoked to understand the formation of *N*-benzoyl-3-methyl-2-azetidinone (see Scheme 2).[20] This radical mechanism starts with a single electron transfer (SET) from the catalyst to the aziridine to give a ketyl radical anion, which in turn evolves to a secondary radical. Then, this species reacts with $Co(CO)_4^{\cdot}$ to afford *N*-benzoyl-3-methyl-2-azetidinone after several rearrangements.

To elucidate the characteristics of the reaction mechanism involved in the CO-catalyzed carbonylative ring expansion of aziridines, we undertook a DFT study of the reaction between *N*-benzoyl-2-methylaziridine and CO catalyzed by the $Co(CO)_4^-$ anion in DME solvent to afford *N*-benzoyl-4-methyl-2-azetidinone and *N*-benzoyl-3-methyl-2-azetidinone, focusing our attention on the regioselectivity and stereospecificity of the process as well. We also investigated the effect of the phenyl and ethyl substituents at the ring C_α carbon atom of aziridine on the regioselectivity of that reaction.

Computational Methods

Quantum chemical computations were carried out with the Gaussian 03 series of programs[31] employing the hybrid density funtional B3LYP,[32−34] which combines Becke's three-parameter nonlocal hybrid exchange potential with the nonlocal correlation functional of Lee, Yang, and Parr. This functional was used with two basis set −ECP (effective core potential) combinations. The first, denoted Base I, is the 6-31+G(d) basis set[35] on the H, C, N, O, and Na atoms with the Stuttgart/Dresden (SDD) basis set−ECP combination on the Co atom.[36] The second, denoted Base II,

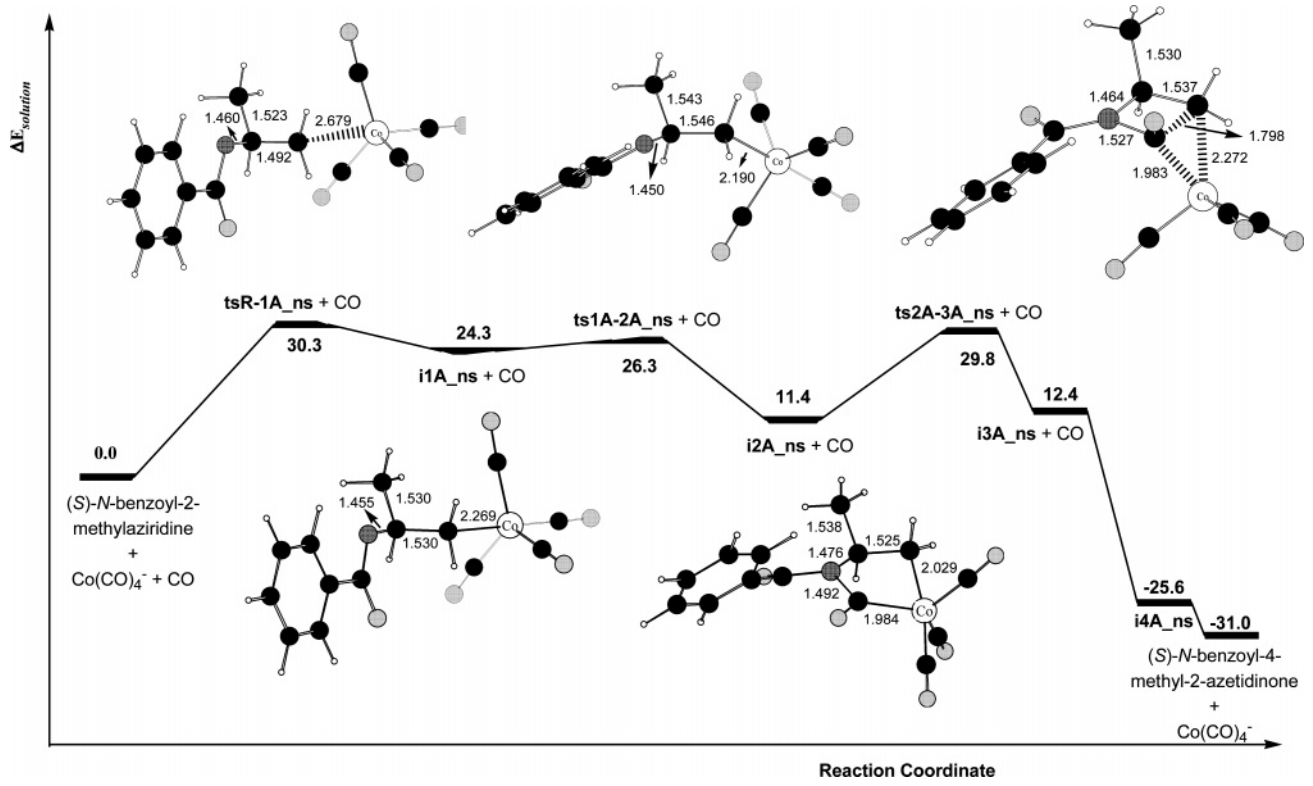

FIGURE 2. B3LYP/Base II/CPCM-UAKS//B3LYP/Base I energy profile (in kcal/mol) in solution of the most favorable reaction mechanism located for the carbonyl attack to the nonsubstituted carbon atom of (*S*)-*N*-benzoyl-2-methylaziridine catalyzed by $Co(CO)_4^-$. Only the most relevant distances (in Å) are displayed.

combines the 6-311++G(d,p) basis set[37] on the nonmetal and Na atoms with the standard SDD basis set−ECP combination augmented by a set of f polarization functions with exponent 2.548 and s, p, d, and f diffuse functions (0.00325, 0.01107, 0.0338, and 0.539, respectively) for the Co atom.[38] Full geometry optimizations of stable species and transition states (TS) were performed in the gas phase by using the B3LYP/Base I level of theory and the standard Schlegel's algorithm.[39] The nature of the stationary points was verified by analytical computations of harmonic vibrational frequencies. Intrinsic reaction coordinate (IRC) calculations with the Gonzalez and Schlegel method have been used to check the two minimum energy structures connecting each TS.[40,41] B3LYP/Base II single-point calculations were also performed on the B3LYP/Base I optimized geometries, which is conventionally denoted as B3LYP/Base II//B3LYP/Base I.

Quantum chemical computations in solution were carried out on gas-phase-optimized geometries at the B3LYP/Base II level of theory using the conductor polarizable continuum model (CPCM)[42,43] of Barone et al. with the united atom Kohm−Sham (UAKS) cavity. This cavity is built up using the united atom topological model (UATM)[44] with radii optimized at the PBE0/6-31G(d) level of theory.[45,46] A recent benchmark study of CPCM with several cavity models reported that the CPCM-UAKS method provided the best estimation of solvation energies for anionic systems.[47] The energy in solution comprises the electronic energy of the polarized solute, the electrostatic solute−solvent interaction energy $<\Psi_f|\mathbf{H}+1/2\mathbf{V}_f|\Psi_f>$, and the nonelectrostatic terms corresponding to cavitation, dispersion, and short-range repulsion. A relative permittivity of 7.20 was assumed in the calculations to simulate DME as the solvent experimentally used.

(31) Frisch, M. J.; Trucks, G. W.; Schlegel, H. B.; Scuseria, G. E.; Robb, M. A.; Cheeseman, J. R.; Montgomery, J. A., Jr.; Vreven, T.; Kudin, K. N.; Burant, J. C.; Millam, J. M.; Iyengar, S. S.; Tomasi, J.; Barone, V.; Mennucci, B.; Cossi, M.; Scalmani, G.; Rega, N.; Petersson, G. A.; Nakatsuji, H.; Hada, M.; Ehara, M.; Toyota, K.; Fukuda, R.; Hasegawa, J.; Ishida, M.; Nakajima, T.; Honda, Y.; Kitao, O.; Nakai, H.; Klene, M.; Li, X.; Knox, J. E.; Hratchian, H. P.; Cross, J. B.; Bakken, V.; Adamo, C.; Jaramillo, J.; Gomperts, R.; Stratmann, R. E.; Yazyev, O.; Austin, A. J.; Cammi, R.; Pomelli, C.; Ochterski, J. W.; Ayala, P. Y.; Morokuma, K.; Voth, G. A.; Salvador, P.; Dannenberg, J. J.; Zakrzewski, V. G.; Dapprich, S.; Daniels, A. D.; Strain, M. C.; Farkas, O.; Malick, D. K.; Rabuck, A. D.; Raghavachari, K.; Foresman, J. B.; Ortiz, J. V.; Cui, Q.; Baboul, A. G.; Clifford, S.; Cioslowski, J.; Stefanov, B. B.; Liu, G.; Liashenko, A.; Piskorz, P.; Komaromi, I.; Martin, R. L.; Fox, D. J.; Keith, T.; Al-Laham, M. A.; Peng, C. Y.; Nanayakkara, A.; Challacombe, M.; Gill, P. M. W.; Johnson, B.; Chen, W.; Wong, M. W.; Gonzalez, C.; Pople, J. A. *Gaussian 03*, revision C.02; Gaussian, Inc., Wallingford CT, 2004.
(32) Becke, A. D. *Phys. Rev. A* **1988**, *38*, 3098.
(33) Lee, C.; Yang, W.; Parr, R. G. *Phys. Rev. B* **1988**, *37*, 785.
(34) Becke, A. D. *J. Chem. Phys.* **1993**, *98*, 5648.
(35) Hehre, W. J.; Radom, L.; Pople, J. A.; Schleyer, P. v. R. *Ab Initio Molecular Orbital Theory*; Wiley: New York, 1986.
(36) Dolg, M.; Wedig, U.; Stoll, H.; Preuss, H. *J. Chem. Phys.* **1987**, *86*, 866.
(37) Krishnan, R.; Binkley, J. S.; Seeger, R.; Pople, J. A. *J. Chem. Phys.* **1980**, *72*, 650.
(38) Iron, M. A.; Lucassen, A. C. B.; Cohen, H.; van der Boom, M. E.; Martin, J. M. L. *J. Am. Chem. Soc.* 2004, *126*, 11699 (Supporting Information Table S2).
(39) Schlegel, H. B. *J. Comput. Chem.* **1982**, *3*, 214.
(40) Gonzalez, C.; Schlegel, H. B. *J. Phys. Chem.* **1989**, *90*, 2154.
(41) Gonzalez, C.; Schlegel, H. B. *J. Phys. Chem.* **1990**, *94*, 5523.
(42) Barone, V.; Cossi, M. *J. Phys. Chem. A* **1998**, *102*, 1995.
(43) Cossi, M.; Scalmani, G.; Rega, N.; Barone, V. *J. Comput. Chem.* **2003**, *24*, 669.
(44) Barone, V.; Cossi, M.; Tomasi, J. *J. Chem. Phys.* **1997**, *107*, 3210.
(45) Perdew, J. P.; Burke, K.; Ernzerhof, M. *Phys. Rev. Lett.* **1996**, *77*, 3865.
(46) Perdew, J. P.; Burke, K.; Ernzerhof, M. *Phys. Rev. Lett.* **1997**, *78*, 1396.
(47) Takano, Y.; Houk, K. N. *J. Chem. Theory Comput.* **2005**, *1*, 70−77.

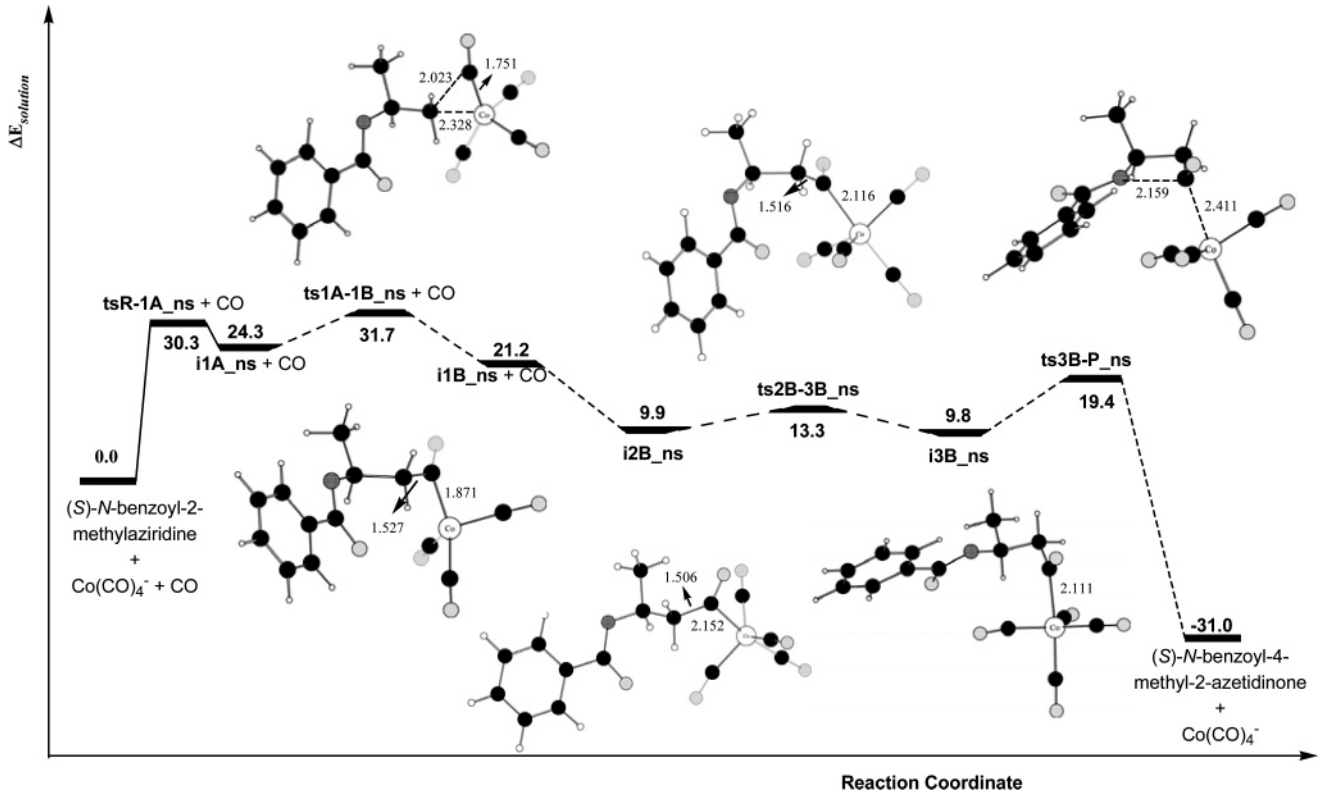

FIGURE 3. B3LYP/Base II/CPCM-UAKS//B3LYP/Base I energy profile (in kcal/mol) in solution of the second most favorable reaction mechanism located for the carbonyl attack to the nonsubstituted carbon atom of (*S*)-*N*-benzoyl-2-methylaziridine catalyzed by $Co(CO)_4^-$. Only the most relevant distances (in angstroms) are displayed.

Results and Discussion

First, we will present the reaction mechanisms found for the $Co(CO)_4^-$-catalyzed carbonylative ring expansion of (*S*)-*N*-benzoyl-2-methylaziridine to (*S*)-*N*-benzoyl-4-methyl-2-azetidinone and then those corresponding to the formation of (*R*)-*N*-benzoyl-3-methyl-2-azetidinone. Tables 1S and 2S in the Supporting Information collect the absolute and relative energies of the structures involved in them, respectively. Second, taking into consideration the obtained results, we will also analyze the effect of the phenyl and ethyl substituents at the carbon α of aziridine on the regioselectivity of the reactive process investigated in this work. Unless otherwise stated, we will give in the text the energy in solution, in parentheses, of all the located species relative to that of the separate reactants, (*S*)-*N*-benzoyl-2-methylaziridine + $Co(CO)_4^-$ + CO.

Reaction Mechanisms. Figure 1 shows an overview of the different reaction mechanisms found for the CO insertion into the C(nonsubstituted)−N bond of (*S*)-*N*-benzoyl-2-methylaziridine and Figure 2 displays the energy profile in solution of the most favorable reaction pathway along with the optimized geometries of the species involved in it (see also Figure 1S in the Supporting Information for reactants and products). In accordance with experimental suggestions,[20,26] the process starts with the attack of $Co(CO)_4^-$ at the backside part of the nonsubstituted C atom of aziridine through the TS **tsR-1A_ns** (30.3 kcal/mol) to give an open intermediate **i1A_ns** (24.3 kcal/mol) in which the metal atom linked now to the attacked C atom presents a trigonal bipypamidal coordination. The Co−C(nonsubstituted) and C(nonsubstituted)−N distances pass from 2.679 and 2.106 Å at **tsR-1A_ns** to 2.269 and 2.333 Å at **i1A_ns**, respectively. **i1A_ns** evolves through the TS **ts1A-2A_ns** (26.3 kcal/mol) for the rotation about the C−C bond of the aziridine moiety with a simultaneous ring closure of the system to give a five-membered cyclic intermediate **i2A_ns**, which is 14.9 kcal/mol more stable than the previous TS. At this intermediate the Co atom presents a trigonal bipyramidal coordination wherein the two Co−C bonds implied in the ring have a length of 1.984 and 2.029 Å. **i2A_ns** leads to another intermediate **i3A_ns** (12.4 kcal/mol) through the TS **ts2A-3A_ns** (29.8 kcal/mol) for the migration of the $Co(CO)_3$ moiety to the initially attacked methylenic carbon atom of aziridine after breaking the two Co−C bonds involved in the five-membered ring and starting to form a new C−C bond that generates the *β*-lactam ring. At this point of the reaction coordinate, we tried to find a TS for an external CO insertion that would give rise to the possibility of recovering the catalyst, but all the searches failed. **i3A_ns** becomes **i4A_ns** (−25.6 kcal/mol) after uptake of an additional CO to complete the coordination sphere of Co to $Co(CO)_4^-$ without encountering any energy barrier. This is in accordance with the obtained theoretical results for the analogous step in the ring expansion of ethylene oxide catalyzed by $BF_3[Co(CO)_4]$.[29] Finally, **i4A_ns** leads to the separate products, (*S*)-*N*-benzoyl-4-methyl-2-azetidinone + $Co(CO)_4^-$ (−31.0 kcal/mol). In the gas phase **i3A_ns**, 35.3 kcal/mol higher in energy than the separate products is already a transient species, but **i4A_ns** is 6.6 kcal/mol more stable than (*S*)-*N*-benzoyl-4-methyl-2-azetidinone + $Co(CO)_4^-$. However, the inclusion of solvent effects in the calculations becomes **i4A_ns** a transient species as well. Figure 2S in the Supporting Information displays the geometries of **i3A_ns** and **i4A_ns**.

All the remaining routes located have in common the first step of the reaction pathway described above (see Figure 1).

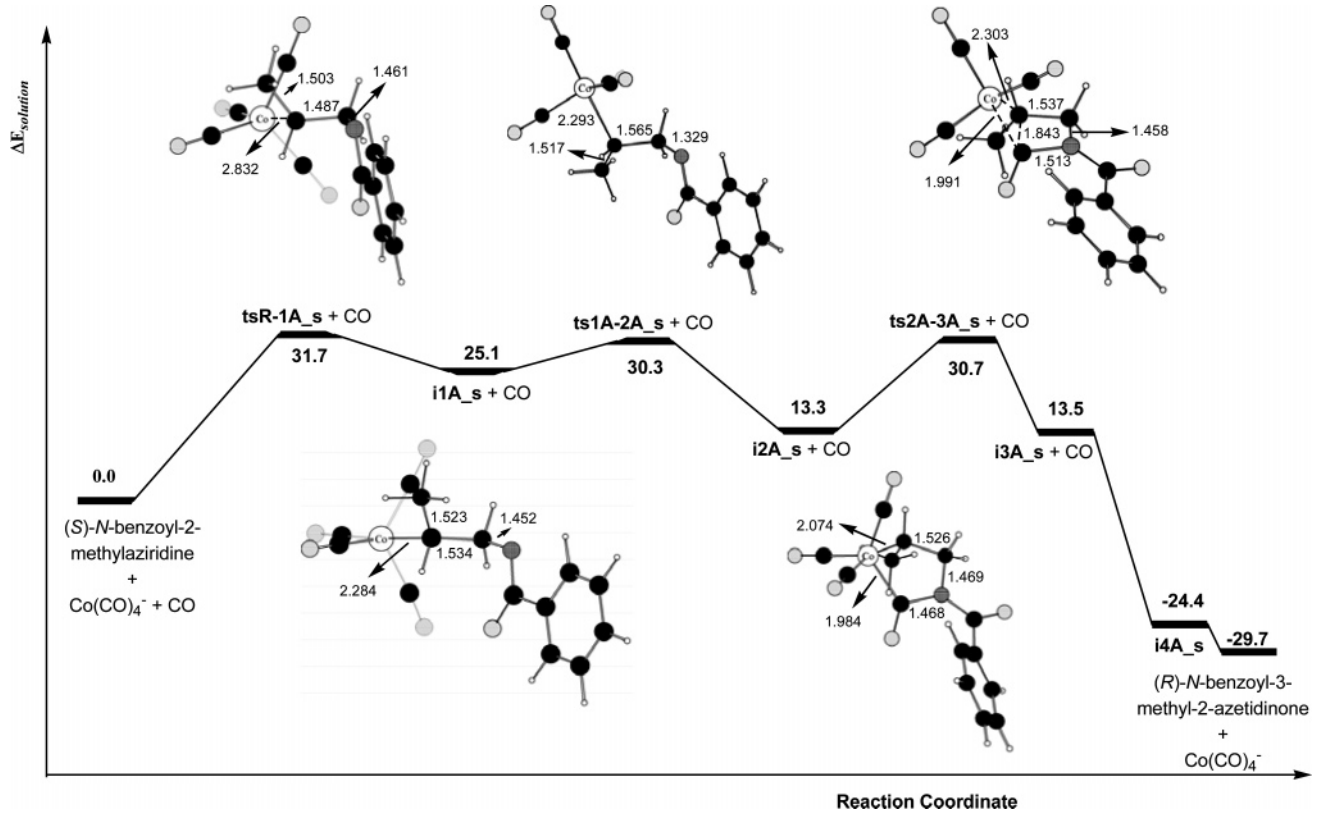

FIGURE 4. B3LYP/Base II/CPCM-UAKS//B3LYP/Base I energy profile (in kcal/mol) in solution of the most favorable reaction mechanism located for the carbonyl attack to the substituted carbon atom of (*S*)-*N*-benzoyl-2-methylaziridine catalyzed by $Co(CO)_4^-$. Only the most relevant distances (in angstroms) are displayed.

The most favorable one of these routes (see Figure 3) evolves through **i1A_ns**, which undergoes an intramolecular insertion of one of the CO ligands of the coordination sphere of metal atom into the Co−C(nonsubstituted) bond to afford the open intermediate **i1B_ns** (21.2 kcal/mol) through the TS **ts1A-1B_ns** (31.7 kcal/mol). At this TS the distance between the attacked C atom and the attacking carbonyl C atom is 2.023 Å while at **i1B_ns** is 1.527 Å, clearly indicating the formation of a new C−C bond. At this intermediate, the metal atom presents a distorted tetrahedral coordination. **i1B_ns** becomes **i2B_ns** (9.9 kcal/mol) after the addition of an external CO to the cobalt atom to regenerate the catalyst without encountering any TS. At this intermediate the metal atom presents again a trigonal bipyramidal coordination. **i2B_ns** evolves to the open intermediate **i3B_ns** (9.8 kcal/mol) through the TS **ts2B-3B_ns** (13.3 kcal/mol) for the rotation about the C−C bond of the aziridine moiety. Finally, **i3B_ns** gives rise to the separate products through the TS **ts3B-P_ns** (19.4 kcal/mol) for the elimination of the catalyst $Co(CO)_4^-$ and simultaneous formation of the *β*-lactam ring. The rate-determining step of this mechanism is the second one with an energy barrier in solution of 31.7 kcal/mol. As can be seen in Figure 1, **i1B_ns** can also become a five-membered cyclic intermediate **i2B'-ns** (2.9 kcal/mol) without encountering any energy barrier through a rotation about the C−C bond of the aziridine moiety and posterior ring closure of the system. Figure 3S collects the optimized geometry of this intermediate and that of the remaining located structures. At **i2B'_ns** the Co atom, which shows a trigonal bipyramidal coordination, is linked to the N atom and to the inserted carbonyl C atom at distances of 2.136 and 1.979 Å, respectively. Instead of any TS for an external CO insertion, we located the TS **ts2B'-3B'_ns** (25.0 kcal/mol) for an intramolecular insertion of one of the CO ligands belonging to the coordination sphere of the metal atom to give a six-membered cyclic intermediate **i3B'_ns** (19.9 kcal/mol), wherein the metal atom recovers the tetrahedral coordination. This intermediate can proceed through two different ways. On one hand, it can give **i2A_ns**, which is one of the intermediates involved in the most favorable reaction mechanism described above, through the TS **ts3B'-2A_ns** (30.1 kcal/mol) thus leading to the separate products as described in Figure 2. This TS corresponds to the cleavage of the bond between the inserted carbonyl C atom and the initially attacked C atom rendering a ring contraction of the system. Although the rate-determining step of this mechanism is again the second one, the system proceeds through higher energies in solution than in the route discussed above. On the other hand, **i3B'_ns** can undergo a CO extramolecular insertion at the Co atom to give the six-membered intermediate **i4B'_ns** (3.1 kcal/mol) through a very unstable TS, **ts3B'-4B'_ns** (45.8 kcal/mol), wherein the distance between Co and the attacking carbonyl C atom is 2.423 Å. This is the only TS located for an external CO insertion. **i4B'_ns** can lead either directly to the separate products, (*S*)-*N*-benzoyl-4-methyl-2-azetidinone + $Co(CO)_4^-$, through the TS **ts4B'-P_ns** (55.3 kcal/mol) for the cleavage of the bond between the initially attacked C atom and the inserted carbonyl C atom or to the above-mentioned intermediate **i3B_ns** (9.8 kcal/mol) through the TS **ts4B'-3B_ns** (12.0 kcal/mol) for the rupture of the C(carbonyl)−N bond. These reaction pathways evolving through **i3B'_ns** to give the products are not competitive due to the existence of high-energy barriers in solution.

In view of the obtained results for the CO insertion into the least substituted C−N bond of (*S*)-*N*-benzoyl-2-methylaziridine

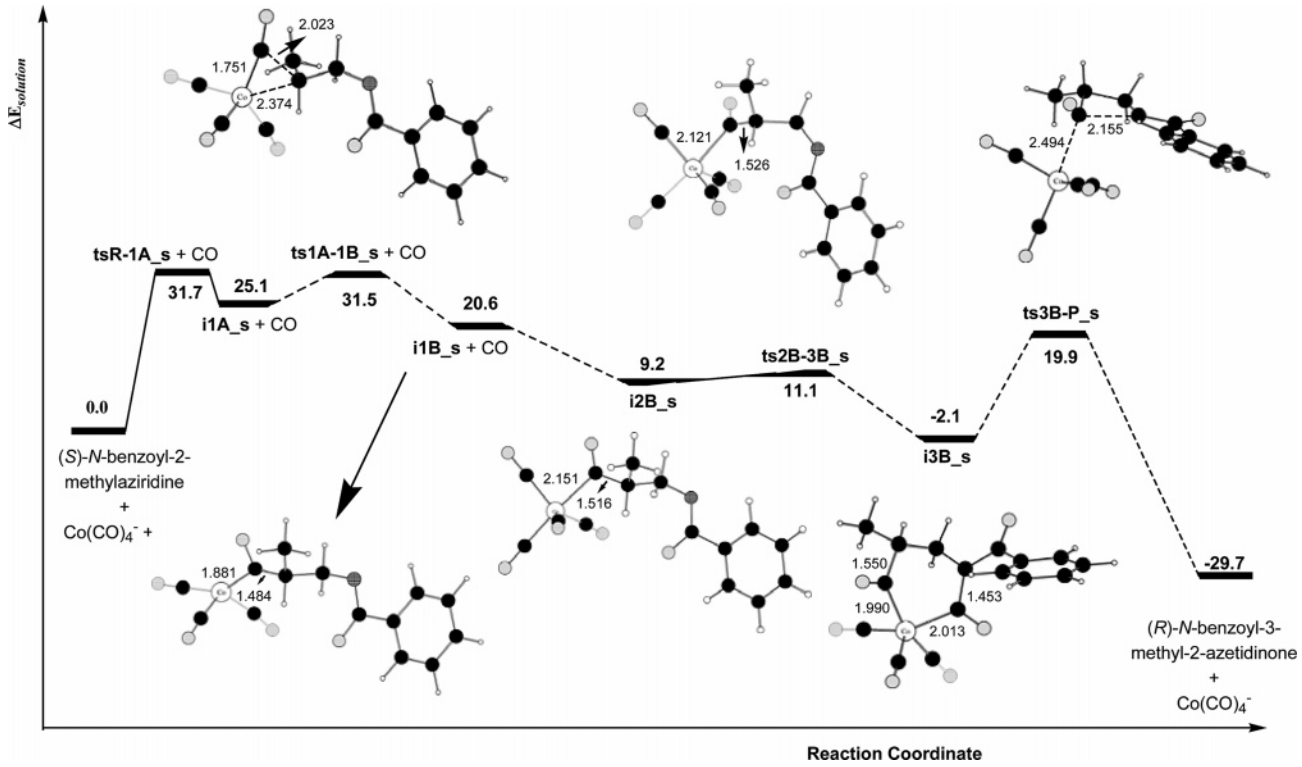

FIGURE 5. B3LYP/Base II/CPCM-UAKS//B3LYP/Base I energy profile (in kcal/mol) in solution of the second most favorable reaction mechanism located for the carbonyl attack to the substituted carbon atom of (*S*)-*N*-benzoyl-2-methylaziridine catalyzed by Co(CO)$_4^-$. Only the most relevant distances (in angstroms) are displayed.

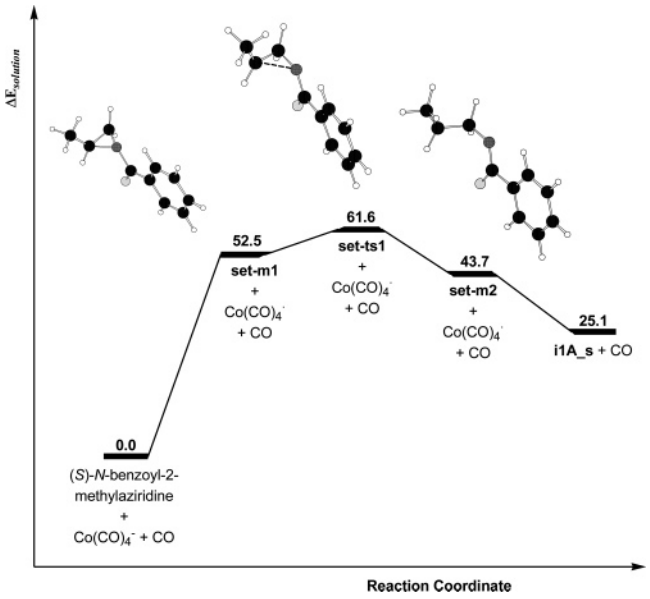

FIGURE 6. UB3LYP/Base II/CPCM-UAKS//UB3LYP/Base I energy profile (in kcal/mol) in solution of the rate determining step of the SET type mechanism located for the carbonyl attack to the substituted carbon atom of (*S*)-*N*-benzoyl-2-methylaziridine catalyzed by Co(CO)$_4^-$.

catalyzed by Co(CO)$_4^-$ to give (*S*)-*N*-benzoyl-4-methyl-2-azetidinone, we only investigated the two most favorable routes for the CO insertion into the most substituted C−N bond of aziridine to give (*R*)-*N*-benzoyl-3-methyl-2-azetidinone. The optimized geometries and energies in solution corresponding to the critical points located for this attack are practically analogous to those displayed in Figures 2 and 3 for the attack discussed above. Figures 4 and 5 shows the corresponding energy profiles in solution and geometrical data of the species involved in them. The TS **tsR-1A_s** (31.7 kcal/mol) for the nucleophilic attack of the catalyst at the backside part of the substituted carbon atom of the aziridine ring is now the rate-determining step of the two most favorable routes and gives rise to an open intermediate **i1A_s** (25.1 kcal/mol). In the most favorable pathway (see Figure 4), this intermediate evolves through the TS **ts1A-2A_s** (30.3 kcal/mol) for the rotation about the aziridine C−C bond with a simultaneous ring closure of the system to give a five-membered cyclic intermediate **i2A_s** (13.3 kcal/mol). This intermediate renders the separate products, (*R*)-*N*-benzoyl-3-methyl-2-azetidinone + Co(CO)$_4^-$ (−29.7 kcal/mol), through the TS **ts2A-3A_s** (30.7 kcal/mol) for the migration of the Co(CO)$_3$ species to the attacked carbon atom and subsequent uptake of an external CO molecule to the cobalt atom followed by the recovering of the catalyst. As in the attack of the catalyst to the nonsubstituted carbon atom for the second most favorable route, **i1A_s** can also undergo an intramolecular insertion of one of the CO ligands of the Co coordination sphere into the aziridine C(substituted)−N bond (**i1B_s**, 20.6 kcal/ mol) followed by an external CO addition to the Co atom to give the intermediate **i2B_s** (9.2 kcal/mol) (see Figure 5). Then, the process proceeds through a rotation about the aziridine C−C bond with a simultaneous ring closure (**i3B_s**, −2.3 kcal/mol) that finally evolves to the separate products. We wish to remark here that the cyclic structure **i3B_s** is analogous to **i4B'_ns**.

No open intermediate analogous to **i3B_ns** was found for this kind of attack. It is also interesting to note that the attacked carbon atom of aziridine bears now the methyl substituent and consequently the step for the rotation about the C−C bond

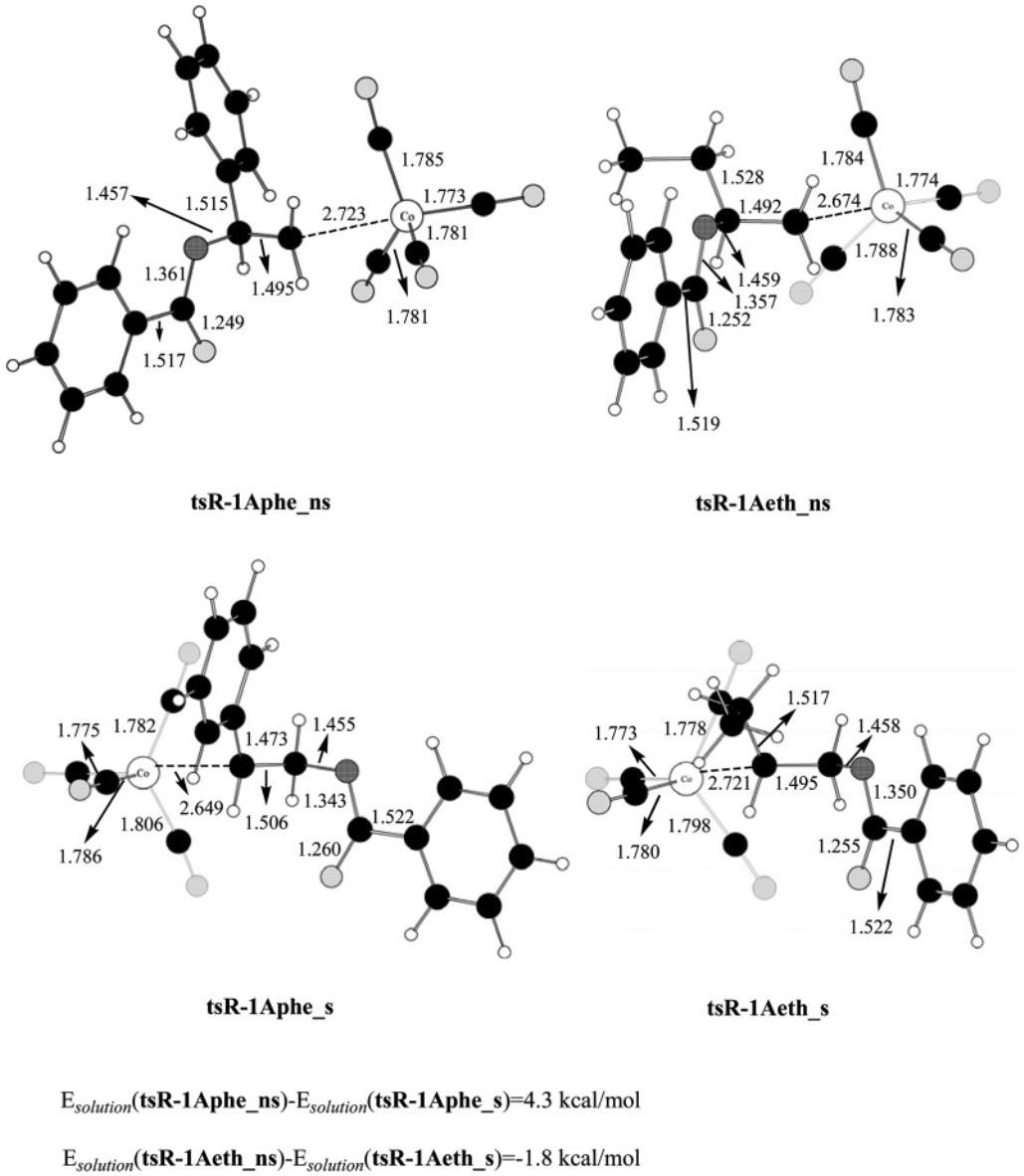

FIGURE 7. B3LYP/Base I-optimized geometries of the TSs corresponding to the aziridine ring opening by the backside attack of $[Co(CO)_4]^-$ at the nonsubstituted and substituted carbon atoms of (*S*)-*N*-benzoyl-2-phenylaziridine and (*S*)-*N*-benzoyl-2-ethylaziridine. Distances are given in angstroms. Relative B3LYP/Base II/CPCM-UAKS//B3LYP/Base I energies for each aziridine are also shown.

originates the inversion of configuration of this stereocenter, thus explaining the formation of (*R*)-*N*-benzoyl-3-methyl-2-azetidinone.

We also investigated the formation of (*R*)-*N*-benzoyl-3-methyl-2-azetidinone following the previously proposed SET mechanism (see Scheme 2).[20] As can be seen in Figure 6, our results[48] show that the SET from $Co(CO)_4^-$ to (*S*)-*N*-methyl-2-aziridine gives rise to the ketyl radical anion **set-m1** and $Co(CO)_4^{\bullet}$, 52.5 kcal/mol less stable than the separate reactants. Then, **set-m1** evolves through the TS **set-ts1** (61.6 kcal/ mol) to give the open intermediate **set-m2** (43.7 kcal/mol), which in turn reacts with $Co(CO)_4^{\bullet}$ to afford **i1A_s**, which gives rise to the corresponding separate products as shown in Figure 4. This mechanistic route is thus 29.9 kcal/mol less favorable, and not competitive, with respect to the above-discussed in Figure 4.

The regioselectivity experimentally observed in the $Co(CO)_4^-$-catalyzed carbonylative ring expansion of (*S*)-*N*-benzoyl-2-methylaziridine[20] can be explained by our theoretical calculations. According to these, the most favorable reaction path for the formation of (*S*)-*N*-benzoyl-4-methyl-2-azetidinone presents an energy barrier in solution of 30.3 kcal/mol (**ts1A_ns**) while that for the formation of (*R*)-*N*-benzoyl-3-methyl-2-azetidinone is 31.7 kcal/mol (**ts1A_s**). Given that **ts1A_ns** is only 1.4 kcal/mol more stable than **ts1A_s**, two regioisomers could form at 100 °C, although (*S*)-*N*-benzoyl-4-methyl-2-azetidinone will predominate over (*R*)-*N*-benzoyl-3-methyl-2-azetidinone in agreement with the experimental yield of 55:37.[20] The stereospecificity experimentally observed (*trans*-aziridines give *cis*-β-lactams, whereas *cis*-aziridines afford *trans*-β-lactams)[20,22−26] are also reproduced by our calculations due

(48) Radical species were optimized at the UB3LYP/Base I level of theory. Single-point calculations were also performed in gas phase and in solution at the UB3LYP/Base II//B3LYP/Base I level of theory. No significant spin contamination was detected in these calculations.

to the inversion of configuration of the aziridine attacked carbon atom along the most favorable reaction mechanisms found.

Effect of Substituent at the C$_\alpha$ Ring Atom. We analyzed the effect of the phenyl and ethyl substituents at the carbon α of aziridine on the regioselectivity of the title reaction by optimizing the TSs for the attack of catalyst to the substituted and nonsubstituted C atoms of aziridine. Figure 4 displays the corresponding geometries and the relative energy difference in solution for each substituent. In the phenyl case, the difference in stability between **tsR-1Aphe_ns** and **tsR-1Aphe_s** is 4.3 kcal/mol, thus giving solely the β-lactam corresponding to the CO insertion into the C(substituted)−N bond of aziridine, (*R*)-*N*-benzoyl-3-phenyl-2-azetidinone. When the phenyl substituent is replaced by the ethyl one, the TS **tsR-1Aeth_ns** for the CO insertion into C(nonsubstituted)−N bond is now the preferred one by 1.8 kcal/mol (1.4 kcal/mol in the case of the methyl substituent), which would give a mixture of (*S*)-*N*-benzoyl-4-ethyl-2-azetidinone and (*R*)-*N*-benzoyl-3-ethyl-2-azetidinone the former being predominant.The significant energy difference found in the case of phenyl substituent is due to the different orientations of the phenyl substituent with respect to the aziridine C−C bond at **tsR-1Aphe_ns** and **tsR-1Aphe_s**. At the former TS the phenyl ring is oriented perpendicularly to the C−C bond, while at the late TS the steric repulsion caused by the approach of Co(CO)$_4^-$ to interact with the substituted carbon atom of aziridine brings about a change in the orientation of the phenyl ring, thus explaining its position along the C−C bond and favoring its interaction with the C(substituent)−N bond that cleaves. This kind of interaction has recently been triggered as a hyperconjugation interaction in a theoretical study on the carbonylative ring expansion of *N*-*tert*-butyl-2-phenylaziridine catalyzed by [Rh(CO)$_2$Cl]$_2$.[30] It is also interesting to note that the replacement of the methyl substituent by the ethyl one rises 0.4 kcal/mol the relative stability of the two TSs implied in the nucleophilic attack of Co(CO)$_4^-$ to the two carbon atoms of aziridine, thus increasing the yield of (*S*)-*N*-benzoyl-4-alkyl-2-azetidinone in the final mixture of β-lactams.

Conclusions

Our theoretical results indicate that the CO insertion into each of the two C−N bonds of *N*-benzoyl-2-methylaziridine catalyzed by Co(CO)$_4^-$ takes place via several reaction mechanisms having in common the first step, which corresponds to the ring opening of aziridine by the backside attack of the Co(CO)$_4^-$ anion. From here, the most favorable reaction mechanism evolves through a rotation about the aziridine C−C bond with a simultaneous ring closure of the system and then a ring contraction to give the β-lactam and recover the catalyst. For both sites of attack the first step is the rate-determining one with an energy barrier in solution of 30.3 kcal/mol for the CO insertion into the aziridine C(nonsubstituted)−N bond and of 31.7 kcal/mol for that into the aziridine C(substituted)−N bond. The energy difference between these two barriers explains the experimental detection of a mixture of the products, *N*-benzoyl-4-methyl-2-azetidinone and *N*-benzoyl-3-methyl-2-azetidinone, the former being predominant. Our results permit us to explain not only the obtaining of the major product but also that of the minor one in contrast with experimental suggestions, which invoked the participation of a radical mechanism. Moreover, the location of a TS for the rotation about the aziridine C−C bond after the attack of catalyst to the aziridine carbon atom provokes the inversion of its configuration, thus explaining the stereospecificity experimentally reported for the ring expansion of aziridines catalyzed by Co(CO)$_4^-$.

The substitution of the methyl group at the carbon α of aziridine by the ethyl one increases the regioselectivity of the process by favoring the formation of the product corresponding to the CO insertion into the least substituted C−N bond of aziridine. This suggests that the choice of a suitable alkyl substituent could lead to the formation of an only product. When the phenyl group is the substituent at the carbon α of aziridine the regioselectivity of the process changes completely in agreement with experimental findings, the only obtained product corresponds to the CO insertion into the phenyl bearing C−N bond. Therefore, the substitutent at the aziridine C$_\alpha$ atom controls the regioselectivity of the process.

Acknowledgment. We are grateful to the Principado de Asturias (Spain) for financial support (PB02-045).

Supporting Information Available: Absolute and relative electronic energies and Gibbs energies of solvation of all the structures presented in the present work, imaginary vibrational frequencies corresponding to all the located transition states, B3LYP/Base I-optimized structures of some significant structures implied in the carbonyl insertion into both the least and the most substituted aziridine C−N bond, Cartesian coordinates corresponding to all the located structures. This material is available free of charge via the Internet at http://pubs.acs.org.

JO0625249